

Performance Analysis of RIS-Assisted Index Modulation for Terahertz Communications

V. Shiva Bhasakar Rao^{1*} and B. Suribabu Naick²

¹Research Scholar, Department of EECE, GITAM (Deemed to be University), Rushikonda, Visakhapatnam, Andhra Pradesh, India; sivabhaskarrao653@gmail.com

²Department of Electronics and Communication Engineering, GITAM (Deemed to be university), AP, 530045, India; sbhukya@gitam.edu

*Correspondence: V. Shiva Bhasakar Rao; sivabhaskarrao653@gmail.com

ABSTRACT- The significance of Terahertz (THz) communication for the upcoming sixth generation (6G) communications, which offers abundant bandwidth for high-speed data transmission. However, THz frequencies face challenges such as propagation attenuation and molecular absorption that limit their coverage range. To address this issue, the use of reconfigurable intelligent surfaces (RIS) and index modulation (IM) has been proposed to extend coverage and reduce bit error rates (BER) at low transmitted power. This paper introduces a novel RIS-assisted IM system for THz communication, employing semi-definite relaxation (SDR) optimization techniques for passive beam forming at the detector. The proposed system, named PRIS-IM, demonstrates superior performance compared to conventional RIS-IM (CRIS-IM) and conventional IM (CIM) without RIS in THz frequencies. Simulation results illustrate a lower BER at a higher signal to-noise ratio (SNR) achieved by increasing the number of passive elements. Furthermore, the mutual information (MI) of the PRIS-IM system is derived and validated with simulation, and the achievable rate of the PRIS-IM system is improved by increasing the number of transmitting antennas and reflecting elements. Moreover, the PRIS-IM system is analyzed in different channel scenarios and distances. Overall, the proposed system exhibits the potential to significantly enhance the BER and MI performance of THz communication, indicating promising prospects for future wireless networks.

Keywords: Terahertz communication; Reconfigurable intelligent surfaces Index modulation; Bit error rate; Semi-definite relaxation; Mutual information.

ARTICLE INFORMATION

Author(s): V. Shiva Bhasakar Rao and B. Suribabu Naick;

Received: 13/09/2024; **Accepted:** 05/11/2024; **Published:** 30/12/2024;

e-ISSN: 2347-470X;

Paper Id: IJEER 1309-14;

Citation: 10.37391/IJEER.120442

Webpage-link:

<https://ijeer.forexjournal.co.in/archive/volume-12/ijeer-120442.html>



Publisher's Note: FOREX Publication stays neutral with regard to Jurisdictional claims in Published maps and institutional affiliations.

1. INTRODUCTION

Terahertz (THz) communication is an emerging technology that holds great promise for the sixth generation (6G) networks due to its wide bandwidth, huge data rate, and low latency, high making it ideal for ultra-high-speed and massive connectivity applications [7]. To improve the communication range, beamforming is a technique that employs an array of multiple antennas to direct signals in a particular direction, resulting in increased signal strength and an extended communication range [20]. Recently, there has been a surge in the development of intelligent reflecting surfaces (IRS) or reconfigurable intelligent surfaces (RIS). These surfaces are made up of numerous passive reflecting elements that can be adjusted to manipulate the incident signal by imparting a specific phase shift. As a result, they offer significant control over the propagation environment of the signal. By adding incident signals constructively to the

desired direction, RIS improves the signal-to-noise ratio (SNR) of received signals, converting non-line-of-sight (NLoS) components to line-of-sight (LoS) and creating a virtual LoS. Moreover, to mitigate the spreading loss and molecular absorption in THz communication, RIS and index modulation (IM) techniques can be employed.

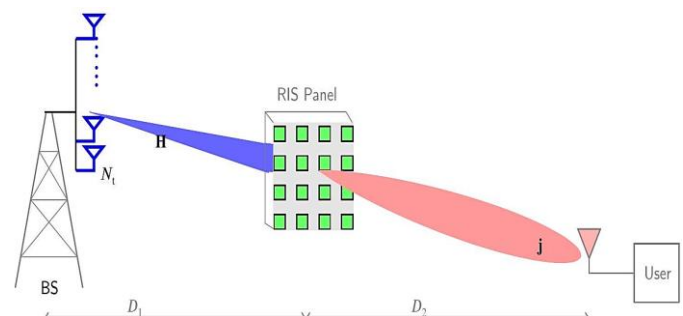


Figure 1. RIS-IM for THz communication system

The combination of RIS and THz communication has been studied extensively in recent literature [1,13] to combat the limitations of spreading loss and molecular absorption. Additionally, the index modulation (IM) technique has been employed to enhance the energy efficiency (EE) of the communication system [3] compare to spatial modulation (SM). IM utilizes the antenna index of the transmitted signal to modulate the signal, reducing the power consumption by decreasing the number of transmitted symbols. Moreover,

various communication systems incorporate this technique, including next-generation wireless communication, where information is transmitted through on/off keying [3]. The RIS-assisted IM technique has been envisioned as a promising solution for THz transmission in 6G networks, this is because it can enhance spectral efficiency (SE) and minimize detection errors.

Recently, several studies have investigated the use of RISs in various aspects of wireless communication. For example, [10] focused on RIS-assisted THz for multiple-input and multiple-output (MIMO) communications and studied the weighted sum-rate. The authors in [9] investigated the performance of RIS at millimeter wave (mm Wave) over fluctuating two rays (FTR) and derived the outage probability. In [12], joint digital and analog beam forming at the base station (BS) and RIS in the THz band were investigated using deep reinforcement learning. The use of IRS for wideband THz communications with holographic reflecting elements was proposed in [8]. Furthermore, [17] analyzed the ergodic capacity for an IRS system in THz transmission. Another study by [4] proposed an RIS assisted transmission through a sub-giga hertz (GHz) band and derived the error probability, which was validated with simulation results. Additionally, [2] proposed RIS to assist with space shift keying (SSK) schemes, EE and SE can be significantly improved, while also analyzing the error probability.

The study of a multi-IRS system in mm Wave/THz communications was presented in [16], where a space-orthogonal scheme was proposed to eliminate inter-user interference (IUI) through zero-forcing techniques. Another study in [17] focused on maximizing the sum-rate of users in THz communications with the assistance of an IRS, using a block coordinate searching algorithm. Additionally, [6] explored the use of an IRS to control the direction of propagation in the THz band, employing an optimization scheme.

The primary contribution of this work is the proposal of a RIS-assisted IM system for THz communication, known as PRIS-IM. The proposed system involves a base station equipped with multiple transmit antennas communicating with a user who has a single antenna using a RIS. The use of RIS enables communication as direct communication between the BS and direct not possible in THz transmission due to high propagation losses and spreading loss. The semi-definite relaxation (SDR) optimization technique is implemented at the detector to reduce the error probability and improve the bit error rate (BER). Furthermore, derived mutual information (MI) for PRIS-IM. Therefore, the achievable rate and coverage area performance can be enhanced while increasing the elements. Moreover PRIS-IM system analyzed in different channel scenario and different distance. Finally, the performance of PRIS-IM is compared with conventional RIS-IM (CRIS-IM) [4] and conventional IM (C-IM) in THz band communications, and the results demonstrate that PRIS-IM provides better performance in entire THz band.

2. PROPOSED SYSTEM MODEL

This section describes the proposed PRIS-IM system for THz band, with the objective of improving the coverage area and reducing the error probability.

2.1 Mathematical Expressions and Symbols

The design of the downlink PRIS-IM system is depicted in *figure 1*. PRIS-IM having BS with N_t transmit antennas that communicates with a single user equipped with a single receive antenna through a reconfigurable intelligent surface (RIS). The RIS consists of a set of N passive reflecting elements that are economical in nature. The distance between the BS and the RIS is denoted by D_1 , whereas the distance between the RIS and the user is represented by D_2 .

The PRIS-IM system encodes data bits $b_t = \log_2(N_t)$ into an index $t \in 1, \dots, N_t$ using the transmitted signals \mathbf{s} from the BS with N_t antennas. The signal is given by:

$$\mathbf{S} = [0, \dots, 0, \underset{\text{at position } t}{1}, 0, \dots, 0]^T \quad (1)$$

Further, base station channel denoted by $\mathbf{H} \in \mathbb{C}^{N \times N_t}$ (BS to RIS.), and RIS channel denoted by $\mathbf{j} \in \mathbb{C}^{N \times 1}$ (RIS to user.), both follow Rician fading distributions [13]. Each channel matrix \mathbf{H} and vector \mathbf{j} can be expressed as the sum of the line-of-sight (LoS) components, denoted by $\tilde{\mathbf{H}}$ and $\tilde{\mathbf{j}}$, respectively, and the non-line-of-sight (NLoS) components, denoted by \mathbf{H} and \mathbf{j} , with Rayleigh flat fading. The power ratio of LoS and NLoS components is represented by Rician factors K_1 and K_2 , respectively. Therefore, the channel matrix \mathbf{H} and \mathbf{j} vector \mathbf{j} are:

$$\mathbf{H} = \left(\sqrt{\frac{K_1}{K_1 + 1}} \tilde{\mathbf{H}} + \sqrt{\frac{1}{K_1 + 1}} \mathbf{H} \right) \in \mathbb{C}^{N \times N_t}, \quad (2)$$

and

$$\mathbf{j} = \left(\sqrt{\frac{K_2}{K_2 + 1}} \tilde{\mathbf{j}} + \sqrt{\frac{1}{K_2 + 1}} \mathbf{j} \right) \in \mathbb{C}^{N \times 1} \quad (3)$$

respectively. The user received signal is expressed as,

$$\mathbf{y} = \mathbf{h}_l [\mathbf{j}^T \Phi \mathbf{H} \mathbf{s}] + \mathbf{w} = \mathbf{h}_l [\mathbf{j}^T \Phi \mathbf{h}_t] + \mathbf{w}, \quad (4)$$

where $\mathbf{h}_t = \mathbf{H} \mathbf{s} \in \mathbb{C}^{N \times 1}$ is the signal transmitted from the activated antennas, and Φ is a diagonal matrix expressed as $\Phi = \text{diag} [\lambda_1 e^{j\phi_1}, \lambda_2 e^{j\phi_2}, \dots, \lambda_N e^{j\phi_N}]$ and $\lambda_n \in (0, 1)$ denotes the amplitude of the n^{th} reflecting element and is assumed to be unity, i.e. $|\lambda_n| = 1 \forall n$ [4]. The $\phi_n \in [0, 2\pi]$, $n = 1, \dots, N$ is the phase of the n^{th} reflecting element, and \mathbf{w} is the additive white Gaussian noise (AWGN) $\sim \mathcal{CN}(0, N_0)$. The h_l denotes the path loss gain at THz. The THz channel path loss is experiences both the spreading loss and molecular absorption is given as, [15],

$$|h_l(D)|_2 = \left(\frac{c}{4\pi f D} \right)^2 e^{-l(f)D} = \zeta D^{-2} e^{-l(f)D} \quad (5)$$

Where ($D = D_1 + D_2$) denotes the overall distance. Additionally, $l(f)$ denotes the molecular absorption

coefficient, as mentioned in [15]. Therefore, the transmitted antenna vector is extracted through the maximum likelihood function (ML) as follows,

$$\hat{t} = \arg \min_{t \in \{1, \dots, N_t\}} \|y - h_t [j^T \Phi h_t]\|_2^2 \quad (6)$$

2.2. Performance analysis of PRIS-IM user

The conditional pair wise error probability (PEP) between transmit antenna index t and incorrectly as \hat{t} is given by Equation 7. This probability is conditioned on H, Φ , and h_t .

$$\Pr(t \rightarrow \hat{t} | H, j, \Phi) = \Pr(|y - h_t [j^T \Phi h_t]|^2 > |y - h_{\hat{t}} [j^T \Phi h_{\hat{t}}]|^2) \quad (7)$$

after substituting y_1 in equation (7), then it follows,

$$\begin{aligned} \Pr(t \rightarrow \hat{t} | H, j, \Phi) &= \Pr(|n|^2 > |h_t [j^T \Phi (h_t - h_{\hat{t}})] + n|^2) \\ &= \Pr(-|h_t [j^T \Phi (h_t - h_{\hat{t}})]|^2 \\ &\quad - 2\Re\{h_t w^* j^T \Phi (h_t - h_{\hat{t}})\} > 0) = \Pr(V > 0) \end{aligned} \quad (8)$$

Where V is Gaussian random variable and its mean and variance is expressed as,

$$E\{V\} = -N \frac{h_t \pi}{4(K+1)} L_{\frac{1}{2}}^2 \left(-\frac{K^2}{K} + 1 \right), \quad (9)$$

$$\text{Var}\{V\} = N h_t^2 \left(1 - \frac{\pi^2}{16(K+1)^2} L_{\frac{1}{2}}^4 \left(-\frac{K^2}{K} + 1 \right) \right). \quad (10)$$

Therefore, conditional PEP is expressed as,

$$\Pr(t \rightarrow \hat{t} | H, j, \Phi) = Q \left(\frac{|h_t [j^T \Phi (h_t - h_{\hat{t}})]|^2}{2N_0} \right) \quad (11)$$

Further, the upper bound of instantaneous error probability is [22],

$$P_e \leq \frac{2}{N_t} \sum_{t=1}^{N_t} \sum_{\hat{t}=1}^{N_t} \Pr(t \rightarrow \hat{t} | H, j, \Phi) \quad (12)$$

$$P_e \leq \frac{2}{N_t} \sum_{t=1}^{N_t} \sum_{\substack{\hat{t}=1 \\ \hat{t} < t}}^{N_t} \Pr(t \rightarrow \hat{t} | H, j, \Phi) \quad (13)$$

where z_{min} can be represented as,

$$z_{min} = \min_{\substack{t, \hat{t} \\ t \neq \hat{t}}} |h_t [j^T \Phi (h_t - h_{\hat{t}})]|^2 \quad (14)$$

Therefore, the error probability (P_e) is minimized by maximizing the z_{min}

$$(P1): \max_{\Phi} z_{min} \quad (15)$$

$$\text{s.t. } \phi_i \in [0, 2\pi], i = 1, \dots, N \quad (16)$$

The problem (P1) is non-convex. Therefore problem (P1) is converted into convex form and optimized by using semi definite relaxation (SDR).

2.3. SDR-based solution

The problem (P1) is converted into (P2) by introducing an auxiliary variable u [14]. The constraints of (P2) are then converted into convex by using a quadratically constraints. The resulting problem (P2) is given as:

$$(P2): \max_{\Phi} u$$

$$\text{s.t. } |h_t [j^T \Phi (h_t - h_{\hat{t}})]|^2 \geq u, \forall t, \hat{t} = 1, \dots, N_t, t \neq \hat{t} \quad (17)$$

$$\phi_i \in [0, 2\pi], \forall i = 1, \dots, N \quad (18)$$

$$|h_t [j^T \Phi (h_t - h_{\hat{t}})]|^2 = |h_t [j^T \text{diag}(h_t - h_{\hat{t}}) \Phi]|^2 \quad (19)$$

$$= \Phi^H W \Phi \quad (20)$$

$$= \text{tr}(W \Phi \Phi^H) \quad (21)$$

The matrix W is defined as $(j^T \text{diag}(h_t - h_{\hat{t}}))^H (j^T \text{diag}(h_t - h_{\hat{t}}))$. We also define $X = \Phi \Phi^H$ subject to the constraint $X \geq 0$, and the rank of X is one. This leads to the problem (P3), which is given as:

$$(P3): \max_X u \quad (22)$$

$$\text{s.t. } \text{tr}(WX) \geq u, \forall t, \hat{t} = 1, \dots, N_t, t \neq \hat{t} \quad (23)$$

$$X_{ii} = 1, \forall i = 1, \dots, N \quad (24)$$

$$X \geq 0 \quad (25)$$

The proposed solution for the problem (P3) involves using a Gaussian randomization scheme. The approach is to apply eigen value decomposition to X , which yields a rank-one solution. This can be expressed as, $X = M \Sigma M^H$, where $M \in \mathbb{C}^{(N+1) \times (N+1)}$ and $\Sigma \stackrel{\Delta}{=} \text{diag}(\sqrt{\xi_1}, \dots, \sqrt{\xi_{N+1}})$. This approach facilitates the effective calculation of problem (P3).

A sub-optimal solution of (P3) by utilizing the following expression $\phi = M \Sigma^{\frac{1}{2}} w$, where w is a random vector with $w \sim \mathcal{CN}(0, I_{N+1})$. The solution of (P3) is approximated by finding the maximum value attained by the best ϕ among all w .

2.4. Mutual information analysis on PRIS-IM system at THZ band

In this subsection, we have derived the mutual information (MI) of the PRIS-IM system. The expression for equation (4) has been reformulated as follows:

$$y = h_t \mathcal{H}_t + w \quad (26)$$

The MI of the PRIS-IM system is determined by $\mathcal{H}_t = [j^T \Phi h_t]$, which exchange the information between the received signal vector space y and the antenna index \mathcal{H}_t . As a result, the MI of the proposed PRIS-IM system for the THz band is, [21]:

$$I(\mathcal{H}_t; y_1) = \int p(y | \mathcal{H}_t) p(\mathcal{H}_t) \times \log_2 \left(\frac{p(y | \mathcal{H}_t)}{\sum_{\mathcal{H}_t} p(y | \mathcal{H}_t) p(\mathcal{H}_t)} \right) dy \quad (27)$$

The variable l is defined in equation (6), and it can be expressed in a different form as:

$$t = \arg \max_t p(y | \mathcal{H}_t) \quad (28)$$

Moreover, $p(y | \mathcal{H}_t)$ represents the conditional probability density function, and it can be defined as follows:

$$p(y | \mathcal{H}_t) = \frac{1}{\pi N_0} \left(e^{-\frac{|y - h_t \mathcal{H}_t|^2}{N_0}} \right) \quad (29)$$

In addition, due to the nature of IM as an erroneous detection scheme, we have $p(\mathcal{H}_t) = N_t$, and by substituting equation (29) into equation (27), we obtain:

$$I(\mathcal{H}_t; y) = \log_2(N_t) - \frac{1}{N_t} \left[\frac{1}{\pi N_0} \sum_t \int e^{-\frac{|y - h_t \mathcal{H}_t|^2}{N_0}} \times \log_2 \left(\sum_t e^{-\frac{|y - h_t \mathcal{H}_t|^2 - |y - h_t \mathcal{H}_t|^2}{N_0}} \right) dy \right] \quad (30)$$

Thus, by performing some algebraic manipulations, equation (30) can be simplified to:

$$I(\mathcal{H}_t; y) = \log_2(N_t) - \log_2(e) - \frac{1}{(N_t)} \sum_t \mathbb{E} \left[\log_2 \left(\sum_t e^{-\frac{|h_t(\mathcal{H}_t - \mathcal{H}_t + w)|^2}{N_0}} \right) \right] \quad (31)$$

3. RESULTS AND DISCUSSION

This section showcases the outcomes of simulation results of PRIS-IM in THz band communication. Along with the parameters, the parameters used in the simulation are also discussed. Further, we assume that carrier frequency is $f = 275\text{GHz}$ with bandwidth is 5GHz [18]. Moreover, THz path gain h_1 is considered as,

$$h_l = \frac{c}{4\pi f(D_1 + D_2)} e^{-\frac{1}{2}l(f)(D_1 + D_2)} e^{-\frac{j2\pi f(D_1 + D_2)}{c}} \text{ with } D_1 = 5\text{m and } D_2 = 30\text{m} [5].$$

We consider the $N_0 = -90\text{dBm/GHz}$ with unit watt transmitted power and Rician factor $K_1 = K_2 = 1$. Figure 2 demonstrates the relationship between the BER and the transmitted power P_t . As the increasing reflecting elements N , the BER performance is improved due to the receiving SNR being directly proportional to N^2 . Furthermore, the PRIS-IM performance outperforms the C-IM since RIS creates a robust LoS from the scattering environment, and the probability of error is inversely proportional to the N^2 .

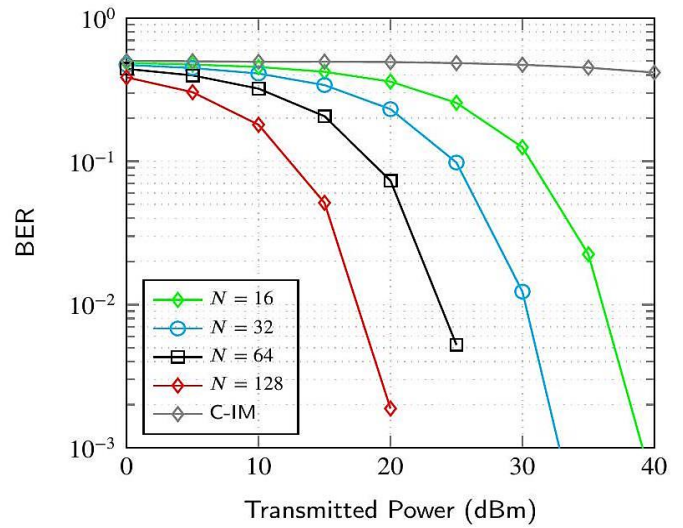


Figure 2. Average BER of PRIS-IM with varying passive reflecting elements N

Figure 3 highlights the minimization of the P_e by maximizing the phase at the ML detector via SDR. As observed from the figure 3, the BER performance of PRIS-IM, achieved with the optimized phase is superior to that obtained with the low complexity detector compare with CRIS-IM [4]. This is due to the maximization of equation (14), which leads to a corresponding decrease in the error.

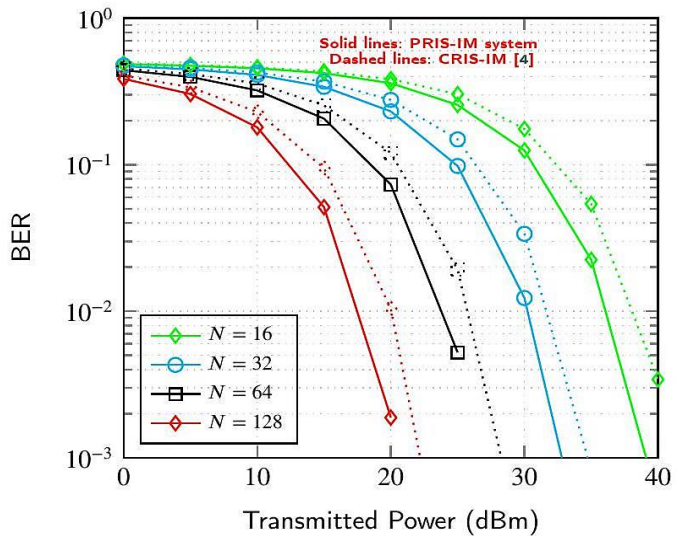


Figure 3. Comparison of average BER of PRIS-IM & CRIS-IM with varying passive reflecting elements N

Next, figure 4 shows the impact of distance D_1 on proposed PRIS-IM system with a fixed reflecting element of $N = 64$ and varying transmit power P_t shows an exponential improvement in BER performance with increasing distance D_1 . This is due to the inverse relationship between the channel path loss gain, h_l , and the received signal strength. As P_t increases, BER is improved. Therefore, our proposed system provides an enhanced coverage area compared to C-IM, which has the worst BER performance.

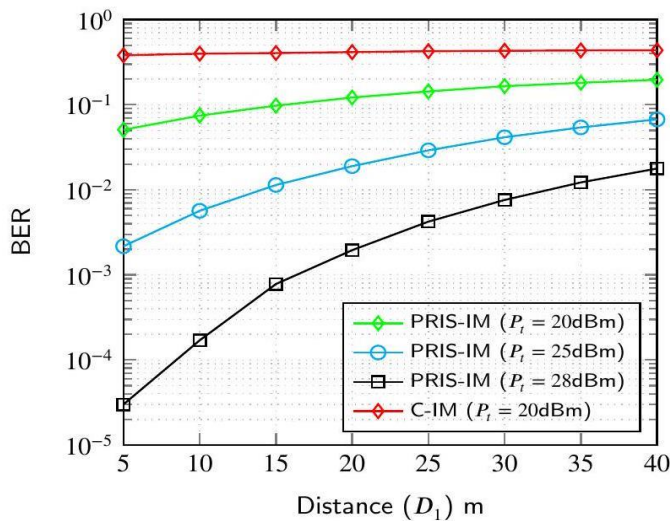


Figure 4. Average BER of PRIS-IM with varying distance D_1

Figure 5, shows the achievable rate of an PRIS-IM system as the transmit power is altered from 0dBm to 40dBm at a carrier frequency of 275GHz. The PRIS-IM system has a fixed transmit antenna with $N_t = 8$ and a varying N . With an increase in the passive elements, the achievable rate enhances, due to an increase in received SNR, which scales as N^2 due to the multiple passive elements that can adjusted to manipulate the incident signals and create virtual LoS. Furthermore, as shown in figure 5, the PRIS-IM is compared with that of conventional index modulation (C-IM) at terahertz frequencies. The comparison demonstrates the superiority of the PRIS-IM system in terms of achievable rate. Additionally, figure 5 provides a comparison between the PRIS-IM system utilizing random phase of the passive elements and the PRIS-IM system utilizing optimized phase of the passive elements. The comparison shows that the optimized phase shifting outperforms the random phase shifting, leading to higher achievable rates for the same reflecting elements. This result emphasizes the significance of optimizing the phase of elements in the RIS to enhance the performance of the system.

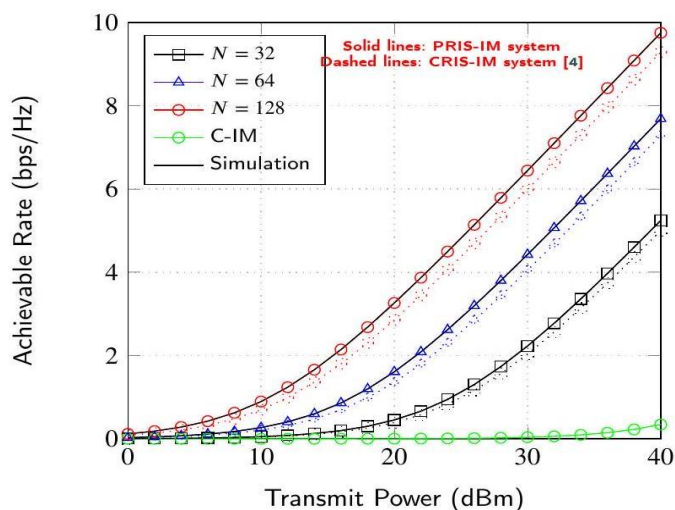


Figure 5. Achievable rate of the PRIS-IM and CRIS-IM system with varying of reflecting elements N & fixed $N_t = 8$

Figure 6 shows that performance of PRIS-IM system improves as the number of transmit antennas, N_t , increases with a fixed number of reflecting elements, $N = 64$. Increasing N_t improves the transmission rate in the IM system, but also enhanced system performance.

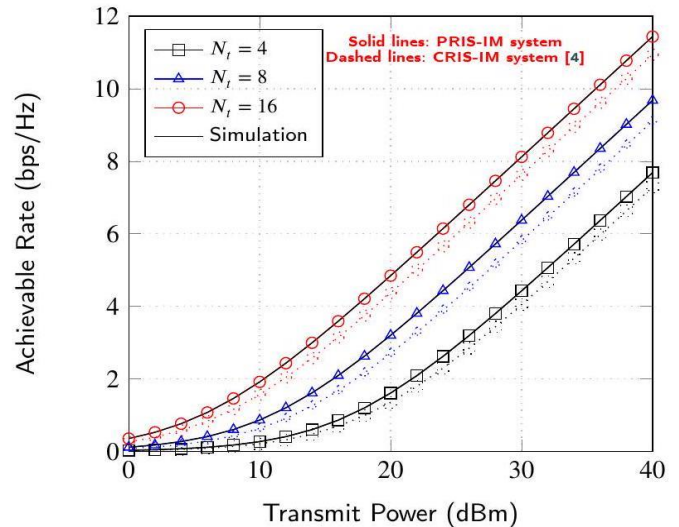


Figure 6. Achievable rate of the PRIS-IM and CRIS-IM system with varying of transmitting antennas N_t & fixed $N = 64$

In addition, the proposed system is compared in Rician and Rayleigh fading channels in figure 7. The Rician factor, K , determines the strength of the LoS component in the channel due RIS is enable. As K increases, the LoS component becomes stronger and the proposed system's performance improves. This is because the LoS component provides a stronger and more reliable signal that can be utilized by the PRIS-IM system to improve the achievable rate.

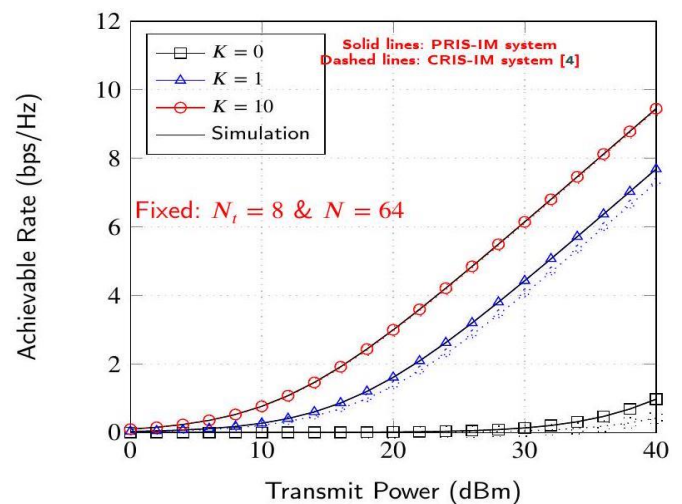


Figure 7. Achievable rate of the PRIS-IM and CRIS-IM system by varying of Rician factor K

Figure 8 illustrates that the achievable rate of the PRIS-IM system deteriorate as the carrier frequency increases, with a fixed elements $N = 64$, transmit antennas ($N_t = 16$), and transmit power P_t . This decrease is due to spreading loss and

molecular absorption, which becomes more significant at higher frequencies in the THz band. However, increasing the transmit power improves the achievable rate.

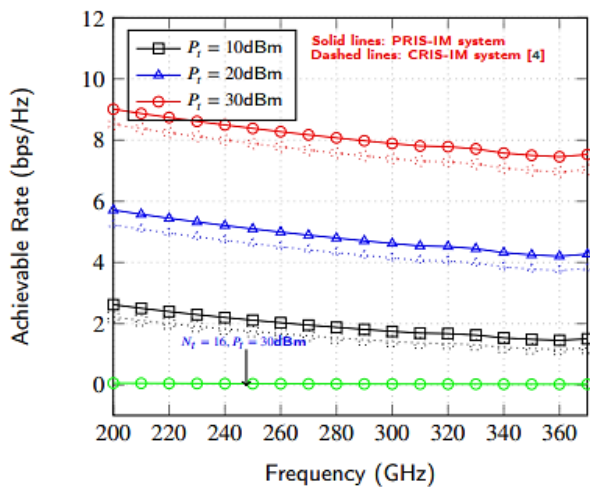


Figure 8. Achievable rate of the PRIS-IM and CRIS-IM system with varying carrier frequency f (in GHz).

4. CONCLUSIONS

In conclusion, the RIS-assisted IM system proposed in this paper showed promising results in improving the coverage area and reducing the probability of errors in THz communication. By utilizing a BS with multiple transmit antennas communicating with a single user through a RIS, the system was able to overcome the high propagation losses and spreading loss characteristic of THz transmission. The semi-definite relaxation optimization technique was used to reduce the error probability and improve the bit error rate. Increasing the passive elements also improved the BER and coverage area performance due to increased diversity order. These results indicate the potential of PRIS-IM in enhancing the performance of THz band. In the future, the proposed system will be further enhanced for multiple users.

Conflicts of Interest: “The authors declare no conflict of interest.”

REFERENCES

- [1] Akyildiz, I.F.; Han, C.; Nie, S., Combating the distance problem in the millimeter wave and terahertz frequency bands, *IEEE Communications Magazine*, 2018, 56, 102–108.
- [2] Basar, E., Reconfigurable intelligent surface-based in demodulation: A new beyond MIMO paradigm for 6G, *IEEE Transactions on Communications*, 2020, 68, 3187–3196.
- [3] Basar, E.; Wen, M.; Mesleh, R.; DiRenzo, M.; Xiao, Y.; Haas, H., Index modulation techniques for next-generation wireless networks. *IEEE access*, 2017, 5, 16693–16746.
- [4] Canbilien, A.E.; Basar, E.; Ikki, S.S., Reconfigurable intelligent surface-assisted space shift keying, *IEEE wireless communications letters*, 2020, 9, 1495–1499.
- [5] Chapala, V.K.; Zafaruddin, S., Exact analysis of RIS-aided THz wireless systems over α - μ fading with pointing errors, *IEEE Communications Letters*, 2021, 25, 3508–3512.
- [6] Chen, Z.; Chen, W.; Ma, X.; Li, Z.; Chi, Y.; Han, C., Taylor expansion aided gradient descent schemes for IRS-enabled terahertz MIMO systems, in: 2020 IEEE Wireless Communications and Networking Conference Workshops (WCNCW), IEEE, pp.1–7.
- [7] Do, H.; Cho, S.; Park, J.; Song, H. J.; Lee, N.; Lozano, A., Terahertz line-of-sight MIMO communication: Theory and practical challenges, *IEEE Communications Magazine*, 2021, 59, 104–109.
- [8] Dovelos, K.; Assimonis, S. D.; Ngo, H. Q.; Bellalta, B.; Matthaiou, M., Intelligent reflecting surfaces at tera hertz bands: Channel modeling and analysis, in: 2021 IEEE International Conference on Communications Workshops (ICC Workshops), IEEE, pp.1–6.
- [9] Du, H.; Zhang, J.; Guan, K.; Ai, B.; Kürner, T.; Reconfigurable intelligent surface aided terahertz communications under misalignment and hardware impairments. *arXivpreprintarXiv:2012.00267*, 2020.
- [10] Hao, W.; Sun, G.; Zeng, M.; Chu, Z.; Zhu, Z.; Dobre, O.A.; Xiao, P.; Robust Design for intelligent reflecting surface-assisted MIMO-OFDMA terahertz IoT networks, *IEEE Internet of Things Journal*, 2021, 8, 13052–13064.
- [11] Huang, C.; Yang, Z.; Alexandropoulos, G.C.; Xiong, K.; Wei, L.; Yuen, C.; Zhang, Z., Hybrid Beamforming for RIS-Empowered Multi-hop Terahertz Communications: A DRL-based Method, in: 2020 IEEE Globe com Workshops IEEE, pp.1–6.
- [12] Kumar, M. H.; Sharma, S.; Deka, K.; Bhatia, V., Intelligent reflecting surface assisted terahertz communications, in: 2022 IEEE International Conference on Signal Processing and Communications (SPCOM), pp.1–5.
- [13] Li, Q.; Wen, M.; Wang, S.; Alexandropoulos, G. C.; Wu, Y. C.; Space shift keying with reconfigurable intelligent surfaces: Phase Configuration designs and performance analysis, *IEEE Open Journal of the Communications Society*, 2021, 2, 322–333.
- [14] Melhem, S. B.; Tabassum, H., User pairing and outage analysis in multi-carrier NOMA-THz networks. *IEEE Transactions on Vehicular Technology*, 2022, 71, 5546–5551.
- [15] Ning, B.; Wang, P.; Li, L.; Chen, Z.; Fang, J., Multi-IRS-Aided Multi-User MIMO in mm Wave/THz Communications: Apace-orthogonal scheme, *IEEE Transactions on Communications*, 2022, 70, 12, pp.8138–8152.
- [16] Pan, Y.; Wang, K.; Pan, C.; Zhu, H.; Wang, J., Sum-rate maximization for intelligent reflecting surface assisted terahertz communications, *IEEE Transactions on Vehicular Technology*, 2022, 71, 3, pp. 3320–3325.
- [17] Polese, M.; Jornet, J.M.; Melodia, T.; Zorzi, M., Toward end-to-end, full-stack 6G terahertz networks, *IEEE Communications Magazine*, 2020, 58, 11, pp.48–54.
- [18] Sameddeen, H.; Saeed, N.; Al-Naffouri, T.Y.; Alouini, M.S., Next Generation Terahertz Communications: A Rendezvous of sensing, imaging, and localization, *IEEE Communications Magazine*, 2020, 58, 69–75.
- [19] Wang, X.; Wang, J.; He, L.; Song, J.; Spectral efficiency analysis for downlink NOMA aided spatial modulation with finite alphabet inputs, *IEEE Transactions on Vehicular Technology*, 2017, 66, pp.10562–10566.
- [20] Yan, W.; Yuan, X.; He, Z.Q.; Kuai, X., Passive beam forming and information transfer design for reconfigurable intelligent surfaces aided multiuser MIMO systems, *IEEE Journal on Selected Area in Communications*, 2020, 38, pp.1793–1808.



© 2024 by the V. Shiva Bhasakar Rao and B. Suribabu Naick. Submitted for possible open access publication under the terms and conditions of the Creative Commons Attribution (CC BY) license (<http://creativecommons.org/licenses/by/4.0/>).